ResearchGate

See discussions, stats, and author profiles for this publication at: https://www.researchgate.net/publication/236333961

On the design and the control of a coupled-inductors boost dc-ac converter for an individual PV panel

Conference Paper · June 2012

DOI: 10.1109/SPEEDAM.2012.6264548

CITATIONS
19

READS
51

5 authors, including:

Marino Coppola
University of Naples Federico II
27 PUBLICATIONS **190** CITATIONS
SEE PROFILE

Santolo Daliento
University of Naples Federico II
92 PUBLICATIONS **625** CITATIONS
SEE PROFILE

Pierluigi Guerriero
University of Naples Federico II
55 PUBLICATIONS **345** CITATIONS
SEE PROFILE

E. Napoli
University of Naples Federico II
149 PUBLICATIONS **1,703** CITATIONS
SEE PROFILE

Some of the authors of this publication are also working on these related projects:

Project Lateral power IGBT devices View project

Project Modeling and design of SuperJunction (SJ) devices View project

All content following this page was uploaded by Pierluigi Guerriero on 17 April 2014.

The user has requested enhancement of the downloaded file.

2012
International Symposium on Power Electronics,
Electrical Drives, Automation and Motion

On the design and the control of a coupled-inductors boost dc-ac converter for an individual PV panel

M. Coppola**, S. Daliento*, P. Guerriero*, D. Lauria**, E. Napoli*
* Dep. of Electronic, and Telecom. Engineering, Univ. of Napoli Federico II, via Claudio 21, 80125 Napoli, (*Italy*)
** Department of Electrical Engineering, Univ. of Napoli Federico II, via Claudio 21, 80125 Napoli, (*Italy*)

Abstract-- **In this paper the design and the control of an individual PV (Photovoltaic) panel dc-ac converter based on a double coupled-inductors boost topology are discussed. The operation principle of the proposed circuit is analyzed. A proper calibration of the PV panel simulation model is performed. An optimization procedure is proposed for choosing the fundamental parameters of both converter and control law based upon sliding control technique. Furthermore, a Maximum Power Point Tracking (MPPT) approach based on a Perturb & Observe (P&O) algorithm is used to track the actual maximum power point through successive approximations. Finally, the proposed inverter is employed as a grid inverter in a single PV panel application. The numerical results reported in the paper permit to confirm the feasibility of the proposed design and control strategy.**

Index Terms-- **coupled-inductors dc-ac converter, sliding mode control, individual photovoltaic panel.**

I. Introduction

Over the last years, the integration of renewable sources in power systems has been developed. This requires also a new regulatory environment which becomes more and more complex for properly ensuring the desired standards of reliability and efficiency.

At the present, the relevant literature is convergent in confirming the potentiality of renewable sources in providing a significant response to the challenge of environmental impact reduction and to the energy crisis. However, studies reinforcements are even requested for tailoring advanced and adequate methodologies and for handling the innovation technology process. The aim is optimal integration of these emerging energy resources in existing electrical distribution systems.

Many renewable resources are characterized by an intrinsic low voltage level, as for example photovoltaic cells, while the distribution network and/or load voltage levels are much higher.

In a conventional PV system many PV modules are connected in series to obtain a dc voltage closed to ac utility line voltage. In this case, PV modules can be affected by partial shadowing effects due to architectural and/or environmental issues. As a consequence, the resulting power generated from the PV array decreases.

At the aim to avoid these drawbacks different approaches based on distributed dc-dc converters [1] or micro-inverter [2]-[4] have been proposed.

This latter solution must provide energy conversion by a boost action both in normal and heavy operating conditions.

Conventional approach to obtain the boost action are: a single stage which use an inverter to generate ac utility line voltage by a step-up transformer; a two stage power generation with a boost dc-dc converter as front stage to get the sufficient dc-bus voltage, and an inverter as second stage to generate the ac utility line voltage. These solutions can result in high volume, weight, cost and reduced efficiency.

The solution proposed in this paper is based on the approach proposed in [5] where the dc-ac conversion is achieved, as shown in Fig. 1, by employing two conventional step-up dc-dc converters and modulating their output voltages in a sinusoidal way.

The boost converters of Fig. 1 produce a dc biased sinusoidal waveform, so that each source generates only a unipolar voltage. The modulation of each converter is 180° out of phase with the other, which maximizes the voltage excursion across the load.

The load is connected between the outputs of each boost converter. Thus, whereas a dc bias appears at each end of the load, with respect to ground, the differential of dc voltage across the load is zero. Generating bipolar voltage at output is solved by a push–pull arrangement. Thus, the dc-dc converters need to be current bidirectional.

As well known, conventional boost converters, due to limitations on the maximum duty cycle, are not able to meet high step-up ratio, while the considered inverter must provide an high voltage amplification of the lower dc input voltage.

An interesting alternative to overcome the latter drawback is the employment of coupled-inductors circuit

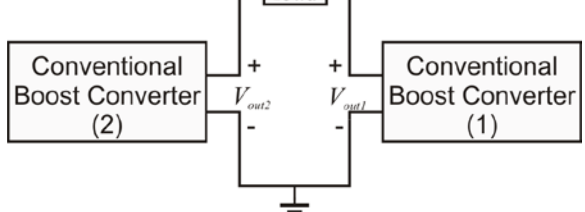

Fig. 1. Double boost dc-ac converter block diagram: the two boost converters produce a dc biased sinusoidal waveform.

978-1-4673-1301-8/12/$31.00 ©2012 IEEE

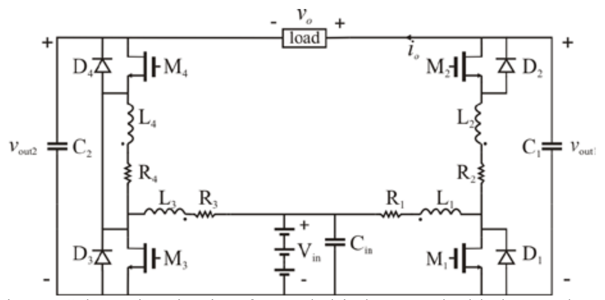

Fig. 2. Schematic circuit of coupled-inductors double-boost dc-ac converter, including copper resistances.

configuration for achieving both high efficiency and high voltage gain [5]-[12].

In this paper the dc-ac converter topology is based on the double-boost circuit proposed in [5] implementing the dc-dc converter with a coupled-inductors boost configuration [3], as depicted in Fig. 2.

The boost action is obtained through a coupled-inductors step-up dc-dc converter, thus exploiting the aforementioned advantages with respect to the conventional circuit.

Unfortunately, a systemic design of coupled-inductor converters is not easy, since many parameters related each other heavily affect the dynamic behavior and the efficiency of the converter. An optimization procedure is proposed for choosing the fundamental parameters of both converter and control law based upon sliding control technique. Sliding mode control has been selected for its well known properties of robustness against disturbances and modeling uncertainties [11].

The micro-inverter proposed in this paper is intended to be used in an individual PV panel power conversion. In such a case, a MPPT (Maximum Power Point Tracking) algorithm provides dynamically the references to the control section in order to assure that the input power is closed to the maximum achievable value.

In particular, the proposed MPPT tracks the actual maximum power point through successive approximations according to Perturb & Observe (P&O) approach [13].

A common problem in P&O algorithms is that the panel operational point is perturbed every MPPT cycle, therefore when the MPP is reached, the output power oscillates around the maximum, resulting in power loss in the PV system. This is especially true in constant or slowly-varying atmospheric conditions but also under rapidly changing atmospheric conditions.

To avoid the oscillation around the MPP, in the optimized P&O technique adopted, the magnitude of the perturbation of the current reference is dynamically weighted with the power-current curve slope. This method allows a better convergence to the actual MPP in terms of precision, avoiding power losses in steady state.

The paper is organized as follows. The system modeling is presented in section II. Hence, section III derives the control law based upon sliding control technique with optimized MPPT algorithm. Section IV is devoted to verify the validity of the proposed design procedure, by performing numerical PSIM simulations. The conclusions are reported in section V.

II. System Modeling

A. Step-up circuit

The ac module shown in Fig. 2 is used to obtain increased voltage gain with respect to the conventional circuit whenever an ac voltage larger than the dc-link voltage is needed (e.g. in grid connected PV power generation). It includes resistors (R_1-R_4) that account for inductors copper losses, the power *MOS* switches (M_1-M_4) and their body diodes (D_1-D_4).

By referring to the right side circuit of Fig. 2, and neglecting the power losses, the dc voltage gain is

$$\frac{V_{out1}}{V_{in}} = \frac{1+ND}{1-D} \tag{1}$$

where $N=N_2/N_1$ is the winding ratio of the magnetically coupled inductors, while N_1 and N_2 are the winding turns of the primary and secondary inductors, and D is the duty cycle. The coupling coefficient, k, is considered ideal ($k=1$). The winding ratio N is a fundamental design parameter in a coupled inductors circuit. The value of N must be properly chosen to maximize the converter efficiency.

The inductance values can be derived as follows:

$$\begin{cases} L_1 = \dfrac{L}{\left(1+N\right)^2} \\ L_2 = \dfrac{N^2}{\left(1+N\right)^2} L = N^2 L_1 \end{cases} \tag{2}$$
$$L = \left(N_1 + N_2\right)^2 L_0$$

where L_0 is the inductance of a single winding and L is the total inductance of the coupled inductors.

The total inductors copper resistance R is split into two contributions:

$$\begin{cases} R_1 = \dfrac{R}{1+N} \\ R_2 = R\dfrac{N}{1+N} \end{cases} \tag{3}$$

Previous considerations are also valid for the left side of the circuit of Fig. 2.

Assuming that the two converters of Fig. 2 are 180° out of phase, the output voltage of the coupled inductors inverter can be easily derived as follows

$$v_o = v_{out1} - v_{out2} = V_{in}\frac{(1+N)(2D-1)}{(1-D)D} \tag{4}$$

then the corresponding voltage gain is

$$\frac{v_o}{V_{in}} = \frac{(1+N)(2D-1)}{(1-D)D} \tag{5}$$

The dc gain characteristic of the boost inverter is depicted in Fig. 3. It is worth highlight that the zero output voltage is obtained for duty cycle, D, equal to *0.5*. If the duty cycle is varied around this point, then an ac voltage appears at the output of the boost inverter [5].

By proper modulation the two converters produce a

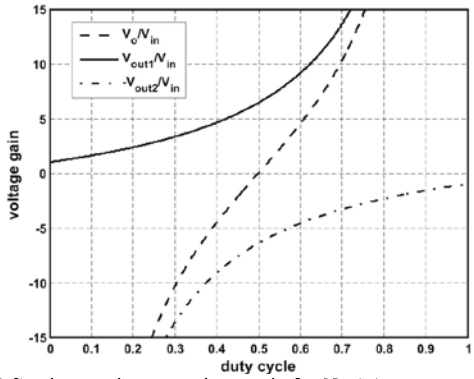

Fig. 3. DC voltage gain versus duty cycle for $N=4.4$.

sinusoidal waveform with a dc bias given by

$$\begin{aligned} v_{out1} &= V_{dc} + A_{pk}\sin(\omega t) \\ v_{out2} &= V_{dc} - A_{pk}\sin(\omega t) \end{aligned} \tag{6}$$

where V_{dc} is the dc bias voltage at each output, while A_{pk} is the ac voltage amplitude added to V_{dc}. Thus, the inverter output voltage can be obtained as

$$v_o = v_{out1} - v_{out2} = 2A_{pk}\sin(\omega t) \tag{7}$$

B. PV panel

The micro-inverter proposed in this paper is intended to be used in an individual PV panel power conversion.

The PV-panel was described through a physical model relying on a generalization of the individual solar cell equivalent lumped electrical circuit (often referred to as five-parameter single-diode model), depicted in Fig. 4, which includes: a current source of photogenerated current I_{ph} (also denoted as photocurrent), an ideal (i.e., resistance-free) diode accounting for the dark *I–V* characteristic – fully defined by the reverse saturation current I_0 and the ideality factor n – and the parasitic shunt and series resistances, denoted with R_{sh} and R_s, respectively.

This popular model, based on the so-called "superposition principle", accurately describes the behavior of most PV panels under standard (i.e., non-stressed) operating conditions.

A calibration procedure was performed to describe the behavior of a commercial PV-panel, which exhibits a nominal power of *160 Wp*, an open-circuit voltage of *36 V* and a short circuit current of *6 A* at STC.

Model input parameters were extracted by analyzing experimental *I-V* curves. In particular, a simple non-intrusive approach was used to accurately assess the shunt resistance and the global series resistance [13-14].

Fig. 5 shows *I-V* (a) and *P-V* (b) curves obtained with the calibrated model at different irradiation levels (*500*, *750* and *1000* W/m^2 respectively).

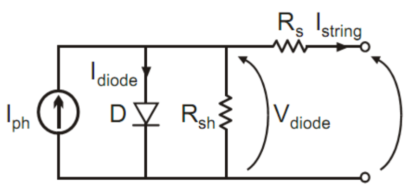

Fig. 4. Individual solar cell five-parameter single-diode model.

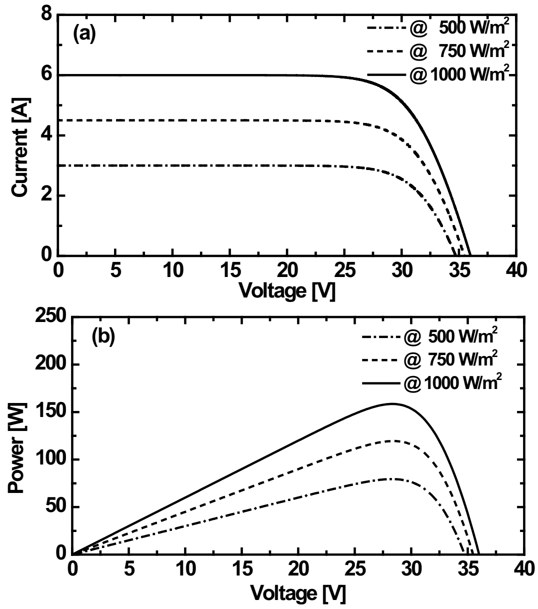

Fig. 5. a) I-V curves obtained with the calibrated model at different irradiation levels: *1000* (solid line), *750* (dotted line) e *500* W/m^2 (dash-dotted line); b) corresponding P-V curves.

III. Control Strategy

The boost inverter of Fig. 2 is composed of the two coupled inductors step-up dc-dc converters. The operation of the overall system can be better understood analyzing the coupled inductors step-up dc-dc converter shown in Fig. 6. For this latter, the sliding mode approach proposed in [11] has been performed.

The first step for modeling the proposed topology of dc-dc converter is the choice of two state space variables. The first one is the output voltage. The second one, since the magnetic flux is not directly measurable, is the current i_{m1}, defined as follows, [7]:

$$i_{m1} = \begin{cases} i_1 & t \in T_{on} \\ i_1(1+N) & t \in T_{off} \end{cases} \tag{8}$$

where, $T_{on}=DT$, $T_{off}=(1-D)T$ and $T=T_{on}+T_{off}$ is the switching time period, N is the turns ratio, as above mentioned, and i_1 is the primary winding current.

By referring to (8) and Fig. 6, the following relationships can be stated:

$$\begin{cases} \dfrac{di_{m1}}{dt} = \dfrac{v_{in} - R_1 i_{m1}}{L_1}u + \dfrac{(v_{in} - v_{out1})}{L_1(1+N)}(1-u) - \dfrac{(R_1+R_2)}{L_1(1+N)^2} i_{m1}(1-u) \\ \dfrac{dv_{out1}}{dt} = \dfrac{i_{m1}}{(1+N)C_1}(1-u) - \dfrac{i_{out1}}{C_1} \end{cases} \tag{9}$$

where $u \in \{0, 1\}$. More specifically, $u=1$ when M_1 is ON (M_2 OFF); $u=0$ when the M_1 is OFF (M_2 ON).

Using the approach proposed in [5], if the vector $\mathbf{x}$ of state-variables error is defined as

$$\mathbf{x} = [x_1, x_2]^T = \left[i_{m1} - I_{m1}^{ref}, v_{out1} - I_{out1}^{ref}\right] \tag{10}$$

the following standard modeling can be deduced

$$\dot{\mathbf{x}} = \mathbf{Ax} + \mathbf{B}u + \mathbf{Az} + \mathbf{F} \tag{11}$$

with $\mathbf{z} = \left[I_{m1}^{ref}, V_{out1}^{ref}\right]^T$

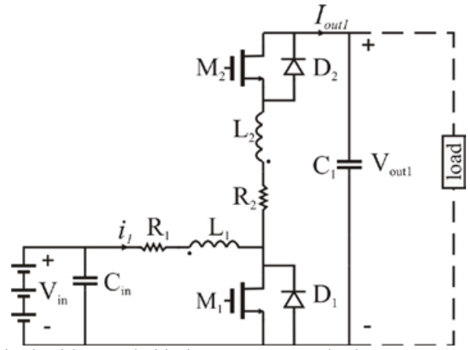

Fig. 6. Single side coupled inductors step-up dc-dc converter.

$$\mathbf{A}=\begin{pmatrix} -\frac{(R_1+R_2)}{L_1(1+N)^2} & -\frac{1}{L_1(1+N)} \\ \frac{1}{(1+N)C_1} & 0 \end{pmatrix}$$

$$\mathbf{B}=\begin{pmatrix} \frac{v_{in}}{L_1}-\frac{R_1}{L_1}i_{m1}-\frac{(v_{in}-v_{out1})}{L_1(1+N)}+\frac{(R_1+R_2)}{L_1(1+N)^2}i_{m1} \\ -\frac{i_{m1}}{(1+N)C_1} \end{pmatrix}$$

$$\mathbf{F}=\begin{pmatrix} \frac{v_{in}}{L_1(1+N)} \\ -\frac{i_{out1}}{C_1} \end{pmatrix}$$

$I_{m1}^{ref}=\frac{1+N}{1-D}I_{out1}^{ref}$.

The reference value of duty ratio is estimated as:

$$D=\frac{1-\frac{v_{in}}{v_{out1}}}{1+N\frac{v_{in}}{v_{out1}}} \tag{12}$$

According to the variable structure system theory, a sliding surface has to be chosen, within the state variables space, where control functions are discontinuous.

The following sliding surface is chosen:

$$S_1(\mathbf{x})=\beta_1 x_1+\beta_2 x_2=\boldsymbol{\beta}^{\mathbf{T}}\mathbf{x} \tag{13}$$

where $\boldsymbol{\beta}^{\mathbf{T}}=[\beta_1,\beta_2]$.

From an heuristic point of view, the optimization procedure for the extraction of the converter and control key parameters proposed in [11] can be used. The assigned input parameters are reported in Table I.

TABLE I

Parameters	Value
Δ	1
C_1	4.4 μF
$v_{in}=V_{in}$	28.3 V
$i_{out1}=I_{out1}$	0.73 A

Δ is an arbitrarily small positive quantity, while 2Δ is the amount of hysteresis in the sliding surface; C_1 is the minimum output capacitance satisfying the constraint on desired output voltage ripple; V_{in} is the maximum power point voltage estimated on the *I-V* characteristic of the used PV panel; and I_{out1} is the desired rms output current.

Table II provides the variables vector values obtained by performing the optimization procedure proposed in [11] on the assumption of negligible state-space errors. The latter means that we can consider (10) $\mathbf{x}\approx 0$ or rather

$$\begin{cases} i_{m1}\simeq I_{m1}^{ref} \iff i_{out1}\simeq I_{out1}^{ref} \\ v_{out1}\simeq V_{out1}^{ref} \end{cases} \tag{14}$$

TABLE II

Parameters	Value
β_1	7.0055
β_2	5.0333
N	4.4
L	6.4 mH
D	0.55

The copper and core losses of the coupled inductor have been considered in conservative way globally equal to 1% of the input power [11]. From Table I and II the total resistance that models copper and core losses can be derived

$$R=49.7\,m\Omega \tag{15}$$

All the above considerations can be replaced for the left side dc-dc converter of the double boost circuit and the same design parameters can be used.

The main purpose of the controllers in Fig. 7 is to make the output voltages v_{out1} and v_{out2} follow as faithfully as possible a sinusoidal reference.

Assuming that the two converters are 180° out of phase, the output voltage references are defined as

$$\begin{aligned} v_{out1}^{ref}&=V_{dc}+\frac{\sqrt{2}A_{rms}}{2}\sin(\omega t+\alpha) \\ v_{out2}^{ref}&=V_{dc}-\frac{\sqrt{2}A_{rms}}{2}\sin(\omega t+\alpha) \end{aligned} \tag{16}$$

where A_{rms} and α are properly chosen by imposing a

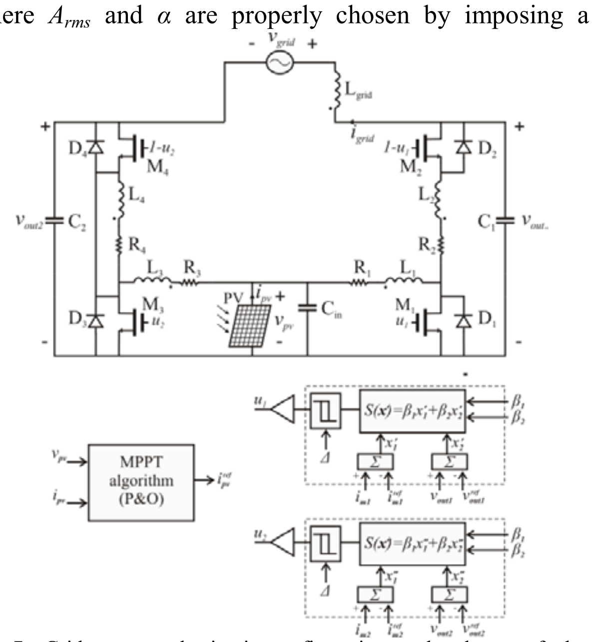

Fig. 7. Grid connected circuit configuration and scheme of the controllers.

unit power factor at the output. Thus, they can be obtained as follows

$$\begin{cases} A_{rms} = \sqrt{V_{grid\,rms}^2 + \left(\dfrac{\omega L_{grid} P_{pv}}{V_{grid\,rms}} \right)^2} \\ \alpha = \arctan\left(\dfrac{\omega L_{grid} P_{pv}}{V_{grid\,rms}^2} \right) \end{cases} \tag{17}$$

The angular frequency ω is the ac grid angular frequency ($\omega=2\pi f$, $f=50\ Hz$), L_{grid} is the grid inductance, and $P_{pv}=v_{pv}i_{pv}$ is the power delivered by the PV panel, which, over the fundamental time period, exhibits low variations at the steady state operating conditions. As suggested in [5], the value of the dc offset (V_{dc}) is chosen to produce a symmetrical variation of the duty cycle around *0.5*. The adopted value is *220 V*, and a variation of the duty cycle between *0.3* and *0.7* is expected, so assuring the operation in the linear zone of the dc gain characteristic depicted in Fig. 3.

Furthermore, the output current references (see Fig. 7) are defined as

$$\begin{aligned} i_{out1}^{ref} &= i_{pv}^{ref} + i_{C1}^{ref} \\ i_{out2}^{ref} &= -i_{pv}^{ref} - i_{C2}^{ref} \end{aligned} \tag{18}$$

The output current reference is the sum of two contributions. The first is in phase with the grid current:

$$i_{pv}^{ref} = A_{MPPT} \sin(\omega t) \tag{19}$$

where A_{MPPT} is obtained through an MPPT algorithm (Fig. 8).

The second is the out of phase current through the output capacitor:

$$i_{C1}^{ref} = \omega C_1 \sqrt{2} \frac{A_{rms}}{2} \sin(\omega t + \alpha + \pi/2) \tag{20}$$

The current references for the sliding mode controllers can be written as follows

$$\begin{cases} i_{m1}^{ref} = \dfrac{1+N}{1-D} i_{out1}^{ref} \\ i_{m2}^{ref} = \dfrac{1+N}{1-D} i_{out2}^{ref} \end{cases} \tag{21}$$

IV. Simulated Performance

The coupled inductors dc-ac converter of Fig. 2 has been designed considering the key circuit parameters listed in Table II, with an output capacitance $C_1=C_2=22\ \mu F$, an input decoupling capacitance $C_{in}=24\ mF$, and a line inductance $L_{grid}=50\ mH$. A PV panel calibrated model has been used as described in sub-section II.B.

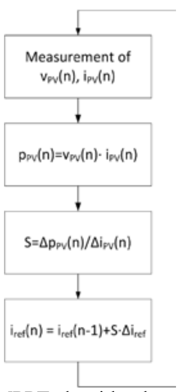

Fig. 8. Flow chart of the MPPT algorithm based on an optimized P&O approach.

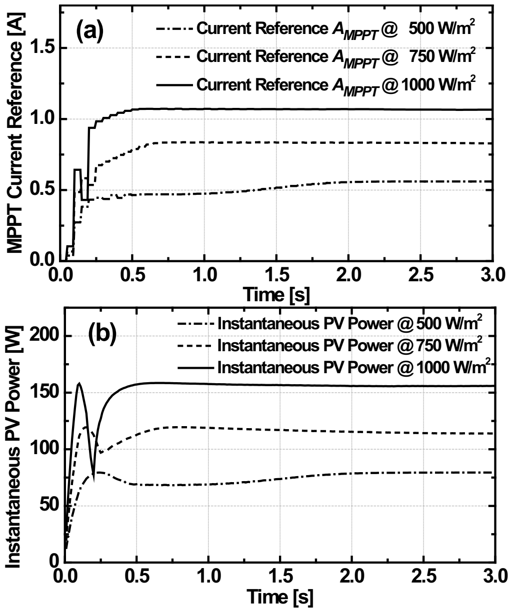

Fig. 9. a) Power current reference vs time for different irradiation levels *1000* (solid line), *750* (dashed line) e *500 W/m²* (dash-dotted line); b) corresponding instantaneous PV power.

At the aim of evaluating PV system performance in terms of MPP tracking a set of simulations have been conducted at different panel irradiation levels (see Fig. 5).

Fig. 9.a) shows the power current reference A_{MPPT} (see eq. 19) dynamically provided by the MPPT algorithm.

The optimized MPPT algorithm is able to guarantee a reduction of the oscillations around the MPP. As a consequence, the MPPT steady-state efficiency is greater than 96% for all the considered cases as shown Fig. 9.b).

Furthermore, the control is able to force the output voltages v_{out1} and v_{out2} to follow the desired 180° out of

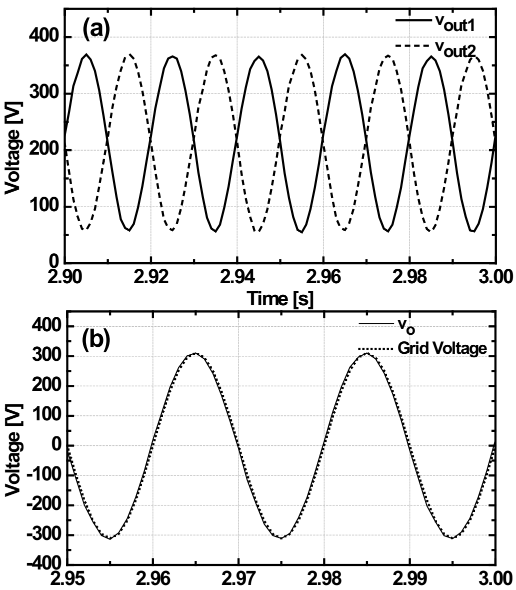

Fig. 10. a) Single side output voltages: v_{out1} (solid line), v_{out2} (dashed line); b) output inverter voltage (solid line) compared to grid voltage (dashed line).

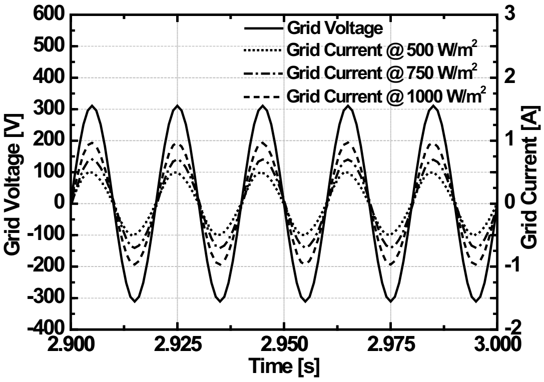

Fig. 11. Grid current at different input power levels (*1000 W/m²*, dashed line; *750 W/m²*, dash-dotted line; *500 W/m²*, dotted line) compared to the grid voltage (solid line).

phase sinusoidal references (eq.16). Fig. 10.a) highlights the steady-state behavior of the single side output voltages, while Fig. 10.b) depicts the inverter output voltage compared to the grid voltage.

The numerical results reported in Fig. 11 investigate the circuit and control performance at different input power levels (i.e. at different irradiation levels). The grid current behavior compared to the grid voltage manifests that the proposed design approach assures a suitable power efficiency.

The estimated efficiency of the inverter is greater than 95.5% for all the above mentioned cases.

V. Conclusions

The paper has focused the attention on the design and the control of a coupled-inductors boost dc-ac converter for an individual PV panel.

A model of the dc-ac converter and the PV panel has been presented. Also, the various aspects concerning both the MPPT and sliding mode control have been discussed in the paper.

Finally, numerical results have been shown to verify the performance of the proposed circuit and control in terms of MPP tracking and overall efficiency.

References

[1] Femia, N., et al. , *"Distributed Maximum Power Point Tracking of Photovoltaic Arrays: Novel Approach and System Analysis"*, IEEE Trans. on Industrial Electronics, vol. 55, no. 7, pp. 2610-2621, 2008.

[2] Haibing Hu, et al. , *"Power decoupling techniques for micro-inverters in PV systems-a review"*, IEEE Energy Conversion Congress and Exposition (ECCE), September 2010, pp. 3235 – 3240.

[3] Fang, Yu; Ma, Xudong, *"A Novel PV Microinverter With Coupled Inductors and Double-Boost Topology"*, IEEE Trans. on Power Electronics, vol. 25, no. 12, pp. 3139-3147, 2010.

[4] Kjaer, S. B., et al. ,*"A Review of Single-Phase Grid-Connected Inverters for Photovoltaic Modules"*, IEEE Trans. on Industry Applications, vol. 41, no. 5, pp. 1292-1306, Sept. 2005.

[5] Caceres, R.O.; Barbi, I., *"A Boost DC-AC Converter: Analysis, Design, and Experimentation"*, IEEE Trans. on Power Electronics, vol. 14, (1), Jan. 1999, pp. 134-141.

[6] Hirachi, K.; Yamanah, M.; Kajiyama, K.; Isokane, S., *"Circuit Configuration of Bidirectional DC/DC Converter Specific for Small Scale Load Leveling System"*, Proc. of the Power Conversion Conf. , Osaka, April 2002, vol. 2, pp. 603-609.

[7] Dwari, S.; Jayawant, S.; Beechner, T.; Miller, S.K.; Mathew, A.; Min Chen; Riehl, J.; Sun, J., *"Dynamics Characterization of Coupled-Inductor Boost DC-DC Converters"*, 2006 IEEE COMPEL Workshop, Troy, NY, USA, July 2006.

[8] Bock, S.A.; Pinheiro, J.R.; Grundling, H.; Hey, H.L.; Pinheiro, H., *"Existence and Stability of Sliding Modes in Bi-directional DC-DC Converters"*, Power Electronics Specialists Conf., PESC. 2001 IEEE 32nd Annual, vol. 3, Vancouver BC, June 2001, pp. 1277-1282.

[9] Ciccarelli, F.; Lauria, D., *"Sliding-mode Control of Bidirectional dc-dc Converter for Supercapacitor Energy Storage Applications"*, IEEE Proc. SPEEDAM, Pisa, May 2010, pp.1119-1122.

[10] Dwari, S.; Parsa, L., *"An Efficient High-Step-Up Interleaved DC-DC Converter With a Common Active Clamp"*, IEEE Trans. On Power Electronics, vol. 26, No. 1, January 2011.

[11] Coppola, M.; Lauria, D.; Napoli, E., *"Optimal Design and Control of Coupled-Inductors Step-Up Dc-Dc Converter"*, IEEE ICCEP, Ischia 2011.

[12] Coppola, M.; Lauria, D.; Napoli, E., *"On the design and the efficiency of coupled step-up dc-dc converters"*, IEEE Proc. ESARS, Bologna, October 2010, pp. 1-6.

[13] d'Alessandro, V., Guerriero, P., Daliento, S., Gargiulo, M., *"Accurately extracting the shunt resistance of photovoltaic cells in installed module strings"*, IEEE ICCEP, Ischia 2011.

[14] d'Alessandro, V.; Guerriero, P.; Daliento, S.; Gargiulo, M., *"A straightforward method to extract the shunt resistance of photovoltaic cells from current-voltage characteristics of mounted arrays"*, Solid-State Electronics, vol. 63, Issue 1, September 2011, pp. 130-136.

View publication stats